QCD static force in gradient flow

Xiang-Peng Wang[1,*]

[1]Physik Department, Technische Universität München, James-Franck-Str. 1, 85748 Garching, Germany

Abstract. We review our recent study on the QCD static force using gradient flow at next-to-leading order in the strong coupling. The QCD static force has the advantage of being free of the $O(\Lambda_{\text{QCD}})$ renormalon appearing in the static potential but suffers from poor convergence in the lattice QCD computations. It is expected that the gradient flow formalism can improve the convergence. Based on our next-to-leading-order calculations, we explore the properties of the static force for arbitrary flow time t, as well as in the limit $t \to 0$, which may be useful for lattice QCD simulations.

1 Motivation

The QCD static potential encodes important information about the QCD interactions for wide range of distances [1–4]. At short distances, the static potential can be calculated perturbatively [3, 5–8] and has been proved to be useful in extracting the strong coupling constant α_s from the latticee QCD simulations [9–14]. The perturbative calculation of the static potential in dimensional regularization suffers a renormalon of order Λ_{QCD}, which may be absorbed in an overall constant shift [15, 16]. Analogously, in lattice regularization, there is a linear divergence that is proportional to the inverse of the lattice spacing.

The static force defined by the spatial derivative of the static potential has the advantage of being free from order Λ_{QCD} rernormalon, which make it more convenient for comparing lattice simulations with perturbative calculations [17–19]. The force can be computed from the finite differences of the lattice data of the static potential, which works well if the available data are dense, like in the case of quenched lattice data [17]. However, at short distances, the lattice data are still sparse, and the computation of the force from their finite differences leads to large uncertainties [10]. An other way of calculating the force is to compute the force directly from a Wilson loop with a chromoelectric field insertion in it [20, 21]. However, direct lattice QCD calculations of the static force exhibit sizable discretization errors and the convergence to the continuum limit is rather slow [22]. This poor convergence may be understood from the convergence of the Fourier transform of the perturbative QCD calculation in momentum space at tree level, in which the spatial momentum integration $\int_0^C d\boldsymbol{q} \cos(\boldsymbol{q}r) = \frac{\sin(Cr)}{r}$ does not converge to a fixed value in the limit $C \to +\infty$, which indicates the the cut off regularization in lattice simulations will face convergence problem in the continuum limit.

The gradient-flow formulation has been proved useful in lattice QCD calculations of correlation functions and local operator matrix elements [23–31]. In gradient flow, the gauge

---

*e-mail: xiangpeng.wang@tum.de

fields in the operator definitions of matrix elements are replaced by flowed fields that depend on the spacetime coordinate and the flow time t. At tree level in perturbation theory, the flowed fields come with a factor $e^{-q^2 t}$ for every momentum-space gauge field with momentum q in the operator definition, which gives an exponential suppression factor at large $\boldsymbol{q}$ in the Fourier transformation. If this suppression behavior is kept unspoiled beyond tree level, we expect that the poor convergence of the lattice QCD calculation of the static force will be greatly improved by using gradient flow.

In this proceeding, we compute the static force in gradient flow in perturbation theory at next-to-leading order in the strong coupling. This calculation is significant in two aspects. First, we examine the convergence of the Fourier transform explicitly beyond tree level. Second, we examine the dependence on the flow time t, and in particular the behavior in the limit $t \to 0$, that may be useful when extrapolating to QCD from lattice calculations done in gradient flow [32].

2 Definitions and conventions

We define the QCD static potential in Euclidean space as [1–4]

$$V(r) = - \lim_{T \to \infty} \frac{1}{T} \log \langle W_{r \times T} \rangle, \tag{1}$$

where $W_{r \times T}$ is a Wilson loop with temporal and spatial extension T and r, respectively, and $\langle \cdots \rangle$ is the color-normalized time-ordered vacuum expectation value

$$\langle \cdots \rangle = \frac{\langle 0 | \mathcal{T} \cdots | 0 \rangle}{\langle 0 | \mathrm{tr}_{\mathrm{color}} \mathbf{1}_{\mathrm{c}} | 0 \rangle}, \tag{2}$$

with $\mathcal{T}$ the time ordering, $|0\rangle$ the QCD vacuum, and $\mathrm{tr}_{\mathrm{color}} \mathbf{1}_{\mathrm{c}} = N_c$ the number of colors. An explicit expression for the Wilson loop $W_{r \times T}$ is

$$W_{r \times T} = \mathrm{tr}_{\mathrm{color}} P \exp \left[ig \oint_C dz^\mu A_\mu(z) \right], \tag{3}$$

where P stands for the path ordering of the color matrices, A_μ is the bare gluon field, g is the bare strong coupling, and C is a closed contour.

We define the QCD static force by the spatial derivative of $V(r)$ as [20–22, 33, 34]

$$F(r) \equiv \frac{\partial}{\partial r} V(r) = -i \lim_{T \to \infty} \frac{1}{T} \frac{\int_{-T/2}^{+T/2} dx_0 \, \langle W_{r \times T} \hat{r} \cdot gE(x_0, r) \rangle}{\langle W_{r \times T} \rangle}, \tag{4}$$

where in the second equality, the chromoelectric field gE_i is inserted into the Wilson loop at spacetime point (x_0, r).

The static force in gradient flow, $F(r; t)$, can be defined by replacing the gluon fields $gA_\mu(x)$ by the flowed fields $B_\mu(x; t)$, where B_μ is defined through the flow equation [25, 26]

$$\frac{\partial}{\partial t} B_\mu(x; t) = D_\nu G_{\nu\mu} + \lambda D_\mu \partial_\nu B_\nu, \; G_{\mu\nu} = \partial_\mu B_\nu - \partial_\nu B_\mu + [B_\mu, B_\nu], \; D_\mu = \partial_\mu + [B_\mu, \cdot], \tag{5}$$

with the initial condition

$$B_\mu(x; t = 0) = gA_\mu(x). \tag{6}$$

Here, λ is an arbitrary constant, and the flow time t is a variable of mass dimension -2.

For perturbative calculations of the static force, it is advantageous to first compute the static potential in gradient flow, $V(r; t)$, by replacing the gluon fields $gA_\mu(x)$ by the flowed

fields $B_\mu(x; t)$ in the definition of the Wilson loop and choose $\lambda = 1$, and then differentiate with respect to r to obtain $F(r; t)$. Since the contributions from the spatial-direction Wilson lines at the times $\pm T/2$ vanish in the limit $T \to \infty$ in Feynman gauge [35], we will employ the Feynman gauge in the calculation of the static potential. The momentum-space potential $\tilde{V}(\boldsymbol{q})$ is related to the position-space counterpart by

$$V(r) = \int \frac{d^3\boldsymbol{q}}{(2\pi)^3} \tilde{V}(\boldsymbol{q}) e^{i\boldsymbol{q}\cdot\boldsymbol{r}}, \tag{7}$$

which is also valid for the static potential in gradient flow. We neglect contributions to $\tilde{V}(\boldsymbol{q})$ with support only at vanishing spatial momentum $\boldsymbol{q}$, such as the heavy quark/antiquark self-energy diagrams, because they do not contribute to the static force.

It has been shown that the IR divergences cancel in the sum of all Feynman diagrams up to two loops [6, 36], and the UV divergences can be removed by the renormalization of the strong coupling. We adopt dimensional regularization with spacetime dimension $d = 4 - 2\epsilon$ and renormalize the strong coupling in the $\overline{\text{MS}}$ scheme.
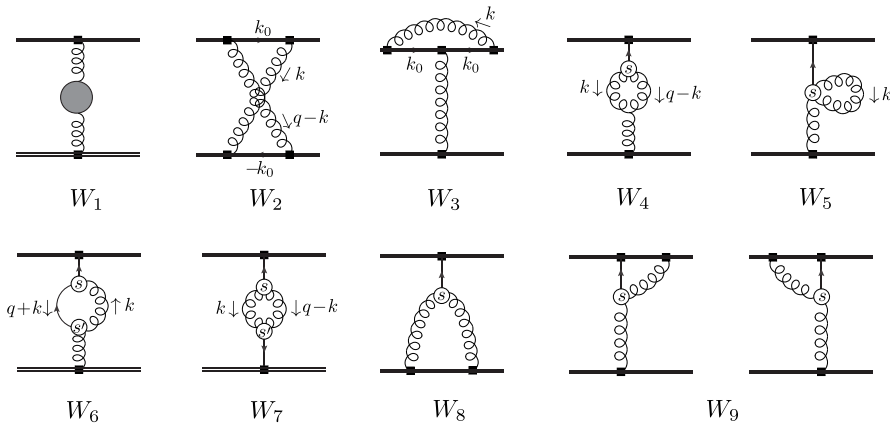
3 Next-to-leading order results

Figure 1. Feynman diagrams for the static potential at next-to-leading order in α_s. The double lines represent temporal Wilson lines, curly lines are gluons, and solid lines are flow lines. Filled squares represent the flowed B_μ fields at flow time t, and open circles are flow vertices. The blob in W_1 represents the gluon vacuum polarization.

In Feynman gauge, the Feynman diagrams for the static potential at next-to-leading order (NLO) in α_s are shown in Figure 1. After renormalization of the strong coupling in the $\overline{\text{MS}}$ scheme, up to order α_s^2, we obtain

$$\tilde{V}(\boldsymbol{q}; t) = -\frac{4\pi\alpha_s(\mu)C_F e^{-2\boldsymbol{q}^2 t}}{\boldsymbol{q}^2}\left\{1 + \frac{\alpha_s(\mu)}{4\pi}\left[\beta_0 \log(\mu^2/\boldsymbol{q}^2) + a_1 + C_A W_{\text{NLO}}^F(\bar{t})\right]\right\}, \tag{8}$$

where $\bar{t} \equiv \boldsymbol{q}^2 t$, $\beta_0 = \frac{11}{3}C_A - \frac{2}{3}n_f$, $a_1 = \frac{31}{9}C_A - \frac{10}{9}n_f$ and $W_{\text{NLO}}^F(\bar{t})$ is finite function of $\bar{t}$. We are not able to obtain full analytical expression for $W_{\text{NLO}}^F(\bar{t})$. Here we only show the numerical results for $e^{-2\bar{t}} W_{\text{NLO}}^F(\bar{t})$ in Figure 2. (See ref. [37] for integration representation of $W_{\text{NLO}}^F(\bar{t})$.)
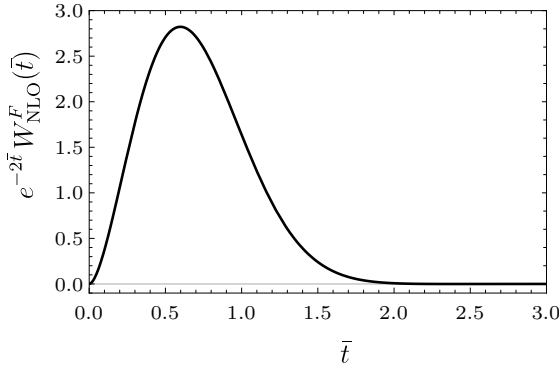
Figure 2. The finite correction term $e^{-2\bar{t}}W_{\text{NLO}}^F(\bar{t})$ as a function of $\bar{t} = \boldsymbol{q}^2 t$.

It is interesting to see the behavior of $W_{\text{NLO}}^F(\bar{t})$ in the limit $\bar{t} \to 0$. And we obtain

$$W_{\text{NLO}}^F(\bar{t}) = \bar{t}\left(-\frac{22\gamma_{\text{E}}}{3} + \frac{277}{18} - \frac{31\log 2}{3} - \frac{22}{3}\log \bar{t}\right) + O(\bar{t}^2). \tag{9}$$

The static force in position space is expressed as

$$F(r;t) = \frac{\partial}{\partial r}\int \frac{d^3\boldsymbol{q}}{(2\pi)^3}\tilde{V}(\boldsymbol{q};t)e^{i\boldsymbol{q}\cdot\boldsymbol{r}} = \frac{1}{r^2}\int_0^\infty d|\boldsymbol{q}|\boldsymbol{q}^2\frac{|\boldsymbol{q}|r\cos(|\boldsymbol{q}|r) - \sin(|\boldsymbol{q}|r)}{2\pi^2|\boldsymbol{q}|}\tilde{V}(\boldsymbol{q};t). \tag{10}$$

We define the following dimensionless quantities

$$\mathcal{F}_0(r;t) = -\int_0^\infty d|\boldsymbol{q}|\boldsymbol{q}^2\frac{|\boldsymbol{q}|r\cos(|\boldsymbol{q}|r) - \sin(|\boldsymbol{q}|r)}{2\pi^2|\boldsymbol{q}|}\frac{4\pi e^{-2\boldsymbol{q}^2 t}}{\boldsymbol{q}^2}, \tag{11}$$

$$\mathcal{F}_{\text{NLO}}^L(r;t;\mu) = -\int_0^\infty d|\boldsymbol{q}|\boldsymbol{q}^2\frac{|\boldsymbol{q}|r\cos(|\boldsymbol{q}|r) - \sin(|\boldsymbol{q}|r)}{2\pi^2|\boldsymbol{q}|}\frac{4\pi e^{-2\boldsymbol{q}^2 t}}{\boldsymbol{q}^2}\log(\mu^2/\boldsymbol{q}^2), \tag{12}$$

$$\mathcal{F}_{\text{NLO}}^F(r;t) = -\int_0^\infty d|\boldsymbol{q}|\boldsymbol{q}^2\frac{|\boldsymbol{q}|r\cos(|\boldsymbol{q}|r) - \sin(|\boldsymbol{q}|r)}{2\pi^2|\boldsymbol{q}|}\frac{4\pi e^{-2\boldsymbol{q}^2 t}}{\boldsymbol{q}^2}W_{\text{NLO}}^F(\bar{t} = \boldsymbol{q}^2 t), \tag{13}$$

so that, up to order-α_s^2,

$$F(r;t) = \frac{\alpha_s(\mu)C_F}{r^2}\left[\left(1 + \frac{\alpha_s}{4\pi}a_1\right)\mathcal{F}_0(r;t) + \frac{\alpha_s}{4\pi}\beta_0\mathcal{F}_{\text{NLO}}^L(r;t;\mu) + \frac{\alpha_s C_A}{4\pi}\mathcal{F}_{\text{NLO}}^F(r;t)\right]. \tag{14}$$

We obtain the behavior of $r^2 F(r;t)$ near $t = 0$ as

$$r^2 F(r;t) \approx r^2 F(r;t = 0) + \frac{\alpha_s^2 C_F}{4\pi}\left[-12\beta_0 - 6C_A c_L\right]\frac{t}{r^2}, \tag{15}$$

where $c_L = -22/3$ is the coefficient of $\bar{t}\log\bar{t}$ in Eq. (9) and $F(r;t = 0)$ is the usual QCD order-α_s^2 result for the static force

$$F(r;t = 0) = \frac{\alpha_s(\mu)C_F}{r^2}\left\{1 + \frac{\alpha_s}{4\pi}\left[a_1 + 2\beta_0\log(\mu r e^{\gamma_{\text{E}}-1})\right]\right\}. \tag{16}$$

Surprisingly, the coefficient of the t/r^2 term is $[-12\beta_0 - 6C_A c_L] = 8n_f$, which vanishes in the pure SU(3) gauge theory ($n_f = 0$).

We show $\mathcal{F}^L_{\mathrm{NLO}}(r; t; \mu)/\mathcal{F}_0(r; t)$ as a function of $r/\sqrt{t}$ in Figure 3 with different choices of renormalization scales. We find that the scale choice $\mu = (r^2 + 8t)^{-1/2}$ makes the logarithmic correction factor $\mathcal{F}^L_{\mathrm{NLO}}(r; t; \mu)/\mathcal{F}_0(r; t)$ of order 1 for all values of $r/\sqrt{t}$. Therefore, we will use $\mu = (r^2 + 8t)^{-1/2}$ here and below for numerical analysis.
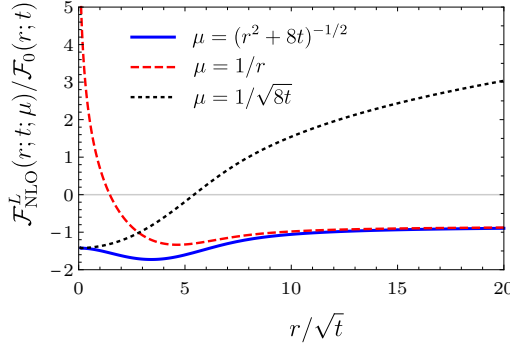

Figure 3. The logarithmic correction factor $\mathcal{F}^L_{\mathrm{NLO}}(r; t; \mu)/\mathcal{F}_0(r; t)$ for $\mu = (r^2 + 8t)^{-1/2}$, $\mu = 1/r$, and $\mu = 1/\sqrt{8t}$ shown as a function of $r/\sqrt{t}$.

Computing α_s in the $\overline{\mathrm{MS}}$ scheme at the scale $\mu = (r^2 + 8t)^{-1/2}$ by using RunDec [38] at four loops, and setting $n_f = 4$, we show the numerical results for the static force in gradient flow, $r^2 F(r; t)$, at NLO in α_s in Figure 4. In the left panel of Figure 4 , we show $r^2 F(r; t)$ as
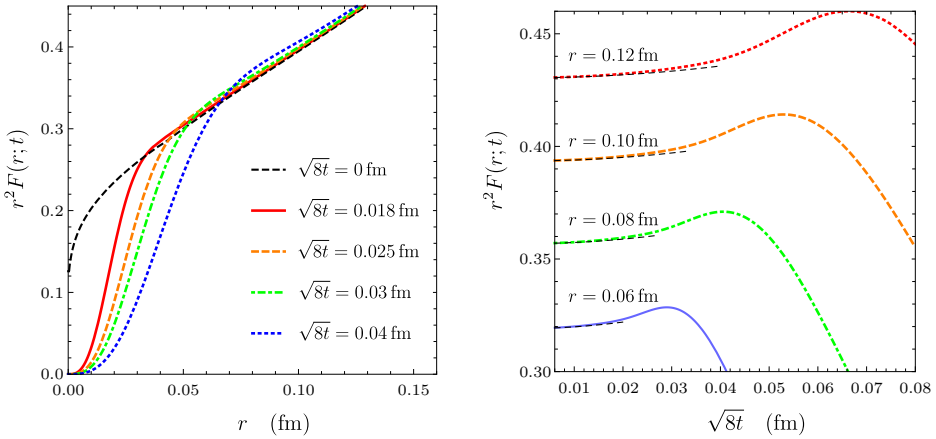

Figure 4. Left panel: numerical results for $r^2 F(r; t)$ for fixed values of $\sqrt{8t}$ as functions of r. Right panel: numerical results for $r^2 F(r; t)$ for fixed values of r as functions of $\sqrt{8t}$; the black dashed lines are approximate results based on Eq. (15), which is valid at small flow time. We have set $\mu = (r^2 + 8t)^{-1/2}$ and $n_f = 4$.

a function of r for several fixed values of $\sqrt{8t}$. We can see that $r^2 F(r; t)$ vanishes for $r \to 0$,

while we recover the QCD result $r^2 F(r; t = 0)$ (black dashed line) for $r \gg \sqrt{8t}$. In the right panel of Figure 4, we show $r^2 F(r; t)$ as a function of t for several fixed values of r. As t decreases, $r^2 F(r; t)$ approaches to the QCD result as expected. We compare the exact NLO result for $r^2 F(r; t)$ at small t with the expression given in Eq. (15) (black dashed lines) in the right panel of Figure 4.
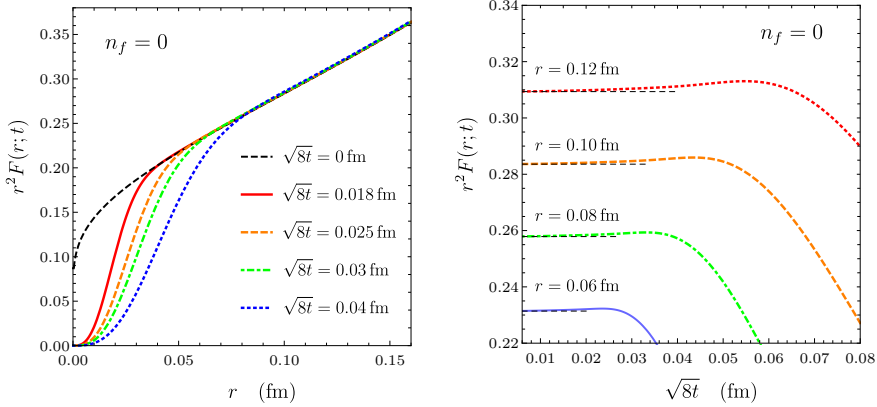

Figure 5. Left panel: numerical results for $r^2 F(r; t)$ in the pure SU(3) gauge theory ($n_f = 0$) for fixed values of $\sqrt{8t}$ as functions of r. Right panel: numerical results for $r^2 F(r; t)$ in the pure SU(3) gauge theory ($n_f = 0$) for fixed values of r as functions of $\sqrt{8t}$; the black dashed lines are the QCD results for $r^2 F(r; t = 0)$. We have set $\mu = (r^2 + 8t)^{-1/2}$.

We also show $r^2 F(r; t)$ in the pure SU(3) gauge theory ($n_f = 0$, quenched case) in Figure 5 as a function of r for fixed values of $\sqrt{8t}$, and as a function of $\sqrt{8t}$ for fixed values of r. We have computed α_s in the pure SU(3) gauge theory by using RunDec [38] at four loops, based on the value $r_0 \Lambda_{QCD} = 0.637^{+0.032}_{-0.030}$ in ref. [39], with $r_0 = 0.5$ fm [17]. Due to the vanishing of the term linear in t in Eq. (15), the expression in Eq. (15) is equal to the QCD result $r^2 F(r; t = 0)$, which we show in the right panel of Figure 5 as horizontal black dashed lines.

4 Summary

In this proceeding, we review our recent study on QCD static force in gradient flow at NLO in the strong coupling. As we have anticipated in the motivation, the gradient flow indeed makes the Fourier transform of the static force in momentum space better converging. Thus we expect that the use of gradient flow may also improve the convergence towards the continuum limit of the lattice QCD simulation of static force done at finite flow time, which is also supported by the results in ref. [32]. Our analytic results of the static force in the limit $t \to 0$ will also be useful when extrapolating to QCD from lattice calculations done in gradient flow. Similar analyses could be extended to a vast range of nonperturbative quarkonium observables in the factorization framework provided by nonrelativistic effective field theories [40]. For instance, one could study in gradient flow the quarkonium potential at higher orders in $1/m$ [33, 41–48], where m is the heavy quark mass, static hybrid potentials [49–51], hybrid potentials at higher orders in $1/m$ [52–54], gluonic correlators entering the expressions of quarkonium inclusive widths and cross sections [55–59].

Acknowledgements

References

[1] K.G. Wilson, Phys. Rev. D **10**, 2445 (1974)

[2] L. Susskind, *Coarse grained Quantum Chromodynamics*, in *Ecole d'Eté de Physique Theorique - Weak and Electromagnetic Interactions at High Energy* (1976), pp. 207–308

[3] W. Fischler, Nucl. Phys. B **129**, 157 (1977)

[4] L.S. Brown, W.I. Weisberger, Phys. Rev. D **20**, 3239 (1979)

[5] Y. Schröder, Phys. Lett. B **447**, 321 (1999), `hep-ph/9812205`

[6] N. Brambilla, A. Pineda, J. Soto, A. Vairo, Phys. Rev. D **60**, 091502 (1999), `hep-ph/9903355`

[7] C. Anzai, Y. Kiyo, Y. Sumino, Phys. Rev. Lett. **104**, 112003 (2010), `0911.4335`

[8] A.V. Smirnov, V.A. Smirnov, M. Steinhauser, Phys. Rev. Lett. **104**, 112002 (2010), `0911.4742`

[9] F. Karbstein, A. Peters, M. Wagner, JHEP **09**, 114 (2014), `1407.7503`

[10] A. Bazavov, N. Brambilla, X.G. Tormo, I, P. Petreczky, J. Soto, A. Vairo, Phys. Rev. D **90**, 074038 (2014), [Erratum: Phys.Rev.D 101, 119902 (2020)], `1407.8437`

[11] F. Karbstein, M. Wagner, M. Weber, Phys. Rev. D **98**, 114506 (2018), `1804.10909`

[12] H. Takaura, T. Kaneko, Y. Kiyo, Y. Sumino, JHEP **04**, 155 (2019), `1808.01643`

[13] A. Bazavov, N. Brambilla, X. Garcia i Tormo, P. Petreczky, J. Soto, A. Vairo, J.H. Weber, Phys. Rev. D **100**, 114511 (2019), `1907.11747`

[14] C. Ayala, X. Lobregat, A. Pineda, JHEP **09**, 016 (2020), `2005.12301`

[15] A. Pineda, Ph.D thesis, University of Barcelona (1998)

[16] A.H. Hoang, M.C. Smith, T. Stelzer, S. Willenbrock, Phys. Rev. D **59**, 114014 (1999), `hep-ph/9804227`

[17] S. Necco, R. Sommer, Nucl. Phys. B **622**, 328 (2002), `hep-lat/0108008`

[18] S. Necco, R. Sommer, Phys. Lett. B **523**, 135 (2001), `hep-ph/0109093`

[19] A. Pineda, J. Phys. G **29**, 371 (2003), `hep-ph/0208031`

[20] A. Vairo, EPJ Web Conf. **126**, 02031 (2016), `1512.07571`

[21] A. Vairo, Mod. Phys. Lett. A **31**, 1630039 (2016)

[22] N. Brambilla, V. Leino, O. Philipsen, C. Reisinger, A. Vairo, M. Wagner (2021), `2106.01794`

[23] R. Narayanan, H. Neuberger, JHEP **03**, 064 (2006), `hep-th/0601210`

[24] M. Lüscher, Commun. Math. Phys. **293**, 899 (2010), `0907.5491`

[25] M. Lüscher, JHEP **08**, 071 (2010), [Erratum: JHEP 03, 092 (2014)], `1006.4518`

[26] M. Lüscher, P. Weisz, JHEP **02**, 051 (2011), `1101.0963`

[27] M. Lüscher, PoS **LATTICE2013**, 016 (2014), `1308.5598`

[28] S. Borsanyi et al., JHEP **09**, 010 (2012), `1203.4469`

[29] H. Suzuki, PTEP **2013**, 083B03 (2013), [Erratum: PTEP 2015, 079201 (2015)], `1304.0533`

[30] H. Makino, H. Suzuki, PTEP **2014**, 063B02 (2014), [Erratum: PTEP 2015, 079202 (2015)], `1403.4772`

[31] R.V. Harlander, Y. Kluth, F. Lange, Eur. Phys. J. C **78**, 944 (2018), [Erratum: Eur.Phys.J.C 79, 858 (2019)], `1808.09837`

[32] V. Leino, N. Brambilla, J. Mayer-Steudte, A. Vairo, EPJ Web Conf. **258**, 04009 (2022), `2111.10212`

[33] N. Brambilla, A. Pineda, J. Soto, A. Vairo, Phys. Rev. D **63**, 014023 (2001), `hep-ph/0002250`

[34] N. Brambilla, V. Leino, O. Philipsen, C. Reisinger, A. Vairo, M. Wagner, PoS **LAT-TICE2019**, 109 (2019), `1911.03290`

[35] Y. Schröder, Ph.D thesis, Hamburg University (1999)

[36] N. Brambilla, A. Pineda, J. Soto, A. Vairo, Nucl. Phys. B **566**, 275 (2000), `hep-ph/9907240`

[37] N. Brambilla, H.S. Chung, A. Vairo, X.P. Wang, JHEP **01**, 184 (2022), `2111.07811`

[38] K.G. Chetyrkin, J.H. Kühn, M. Steinhauser, Comput. Phys. Commun. **133**, 43 (2000), `hep-ph/0004189`

[39] N. Brambilla, X. Garcia i Tormo, J. Soto, A. Vairo, Phys. Rev. Lett. **105**, 212001 (2010), [Erratum: Phys.Rev.Lett. 108, 269903 (2012)], `1006.2066`

[40] N. Brambilla, A. Pineda, J. Soto, A. Vairo, Rev. Mod. Phys. **77**, 1423 (2005), `hep-ph/0410047`

[41] E. Eichten, F.L. Feinberg, Phys. Rev. Lett. **43**, 1205 (1979)

[42] A. Barchielli, N. Brambilla, G.M. Prosperi, Nuovo Cim. A **103**, 59 (1990)

[43] G.S. Bali, K. Schilling, A. Wachter, Phys. Rev. D **56**, 2566 (1997), `hep-lat/9703019`

[44] A. Pineda, A. Vairo, Phys. Rev. D **63**, 054007 (2001), [Erratum: Phys.Rev.D 64, 039902 (2001)], `hep-ph/0009145`

[45] N. Brambilla, A. Pineda, J. Soto, A. Vairo, Phys. Lett. B **580**, 60 (2004), `hep-ph/0307159`

[46] Y. Koma, M. Koma, H. Wittig, Phys. Rev. Lett. **97**, 122003 (2006), `hep-lat/0607009`

[47] Y. Koma, M. Koma, Nucl. Phys. B **769**, 79 (2007), `hep-lat/0609078`

[48] Y. Koma, M. Koma, AIP Conf. Proc. **1322**, 298 (2010)

[49] K.J. Juge, J. Kuti, C. Morningstar, Phys. Rev. Lett. **90**, 161601 (2003), `hep-lat/0207004`

[50] S. Capitani, O. Philipsen, C. Reisinger, C. Riehl, M. Wagner, Phys. Rev. D **99**, 034502 (2019), `1811.11046`

[51] C. Schlosser, M. Wagner (2021), `2111.00741`

[52] R. Oncala, J. Soto, Phys. Rev. D **96**, 014004 (2017), `1702.03900`

[53] N. Brambilla, W.K. Lai, J. Segovia, J. Tarrús Castellà, A. Vairo, Phys. Rev. D **99**, 014017 (2019), [Erratum: Phys.Rev.D 101, 099902 (2020)], `1805.07713`

[54] N. Brambilla, W.K. Lai, J. Segovia, J. Tarrús Castellà, Phys. Rev. D **101**, 054040 (2020), `1908.11699`

[55] N. Brambilla, D. Eiras, A. Pineda, J. Soto, A. Vairo, Phys. Rev. Lett. **88**, 012003 (2002), `hep-ph/0109130`

[56] N. Brambilla, D. Eiras, A. Pineda, J. Soto, A. Vairo, Phys. Rev. D **67**, 034018 (2003), `hep-ph/0208019`

[57] N. Brambilla, H.S. Chung, D. Müller, A. Vairo, JHEP **04**, 095 (2020), `2002.07462`

[58] N. Brambilla, H.S. Chung, A. Vairo, Phys. Rev. Lett. **126**, 082003 (2021), `2007.07613`

[59] N. Brambilla, H.S. Chung, A. Vairo, JHEP **09**, 032 (2021), `2106.09417`